# HCCCH Experiment for Through-Bond Correlation of Thymine Resonances in $^{13}$C-Labeled DNA Oligonucleotides

Vladimír Sklenář,*[,1] James E. Masse,† and Juli Feigon†[,1]

*Department of Chemistry, Faculty of Science, Masaryk University Brno, Kotláøská 2, CZ-611 37 Brno, Czech Republic; and †Department of Chemistry and Biochemistry and Molecular Biology Institute, University of California, Los Angeles, California 90095-1569

**Application of heteronuclear magnetic resonance pulse methods to $^{13}$C,$^{15}$N-labeled nucleic acids is important for the accurate structure determination of larger RNA and DNA oligonucleotides and protein–nucleic acid complexes. These methods have been applied primarily to RNA, due to the availability of labeled samples. The two major differences between DNA and RNA are at the C2′ of the ribose and deoxyribose and the additional methyl group on thymine versus uracil. We have enzymatically synthesized a $^{13}$C,$^{15}$N-labeled 32 base DNA oligonucleotide that folds to form an intramolecular triplex. We present two- and three-dimensional versions of a new HCCCH–TOCSY experiment that provides intraresidue correlation between the thymine H6 and methyl resonances via the intervening carbons (H6–C6–C5–Cme–Hme).** © 1999 Academic Press

The use of $^{13}$C- and/or $^{15}$N-labeled DNA for studying larger oligonucleotide structures and protein–DNA complexes presents obvious advantages over methods that use only $^1$H NMR. In addition to the improvement in assignments, for protein–DNA complexes it should be possible to obtain a better structure for the DNA in the complex. Although a large number of new NMR experiments that exploit the $^{15}$N and $^{13}$C labels in uniformly labeled RNA have been published (*1, 2*), to date few applications to DNA have been reported, due to the relative unavailability of comparably labeled DNA samples. With the recent development of methods of synthesizing labeled DNA enzymatically (*3–7*) and chemically (*8, 9*), it is now possible to begin to apply heteronuclear NMR methods to uniformly $^{13}$C,$^{15}$N-labeled DNA and complexes (*10*).

Most of the magnetization transfer pathways for DNA and RNA are the same, and therefore previously developed methods for obtaining assignments on labeled RNA can be extended in a straightforward way to DNA. The two major differences are at the C2′ of the ribose and deoxyribose and the additional methyl group on thymine versus uracil. Here we present an experiment that provides unambiguous intraresidue correlation between the thymine H6 and methyl resonances via the intervening carbons (H6–C6–C5–Cme–Hme). In smaller DNA oligonucleotides, these connectivities can usually be obtained via

TOCSY (*11, 12*) experiments ($J_{H6,Hme} \sim 1.3$ Hz); however, for larger DNAs and DNA–protein complexes, the relaxation times, especially for $^{13}$C-labeled DNA, may be too short to allow sufficient magnetization transfer times ($>60$ ms) for detection. Since in a regular B–DNA the effective distances H6–Hme(intra) and H6–Hme(inter 5′–>3′) calculated by averaging over three methyl protons are close to 2.9 and 3.2 Å, respectively, both intra- and sequential inter-residual connectivities are observed in NOE or ROE spectra. As a result, the corresponding cross-peaks will have similar intensities. The resolution of these connectivities and their assignments therefore becomes a problem in structures with several *T*'s. In the case of the proposed double-resonance HCCCH experiment the $^{13}$C dimension can be included to allow resolution of overlapping $^1$H cross-peaks for unambiguous assignment. To demonstrate its performance, the HCCCH experiment is applied to a 32 nucleotide uniformly $^{13}$C,$^{15}$N-labeled DNA intramolecular triplex (*13*) (Fig. 1A).

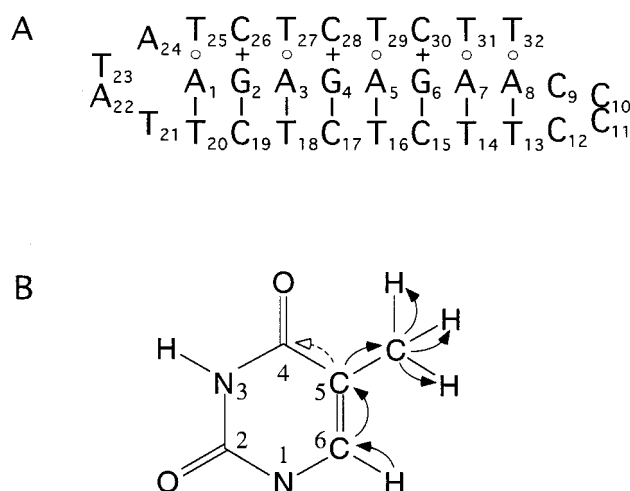The pulse sequence is designed to correlate the H6 and Hme



**FIG. 1.** (A) Sequence and secondary structure of the intramolecular DNA triplex used in these studies. (B) Coherence transfer pathway in thymine. The selected pathway is shown with solid arrows. Unwanted coherence transfer which is eliminated by the experiment is shown with a dashed arrow.

[1] To whom correspondence should be addressed.

**TABLE 1**
**Chemical Shifts and Coupling Constants**
**of Thymine Carbons and Protons**

| $^{13}$C (ppm) | $^{1}$H (ppm) | $J$ (Hz) |
|---|---|---|
| C6 136–140 | H6 7–8 | C6–C5 66 |
| | Hme | |
| C5 110 | 1–2 | C5–Cme 55 |
| Cme 12 | | C6–H6 180 |
| C4 165–170 | | Cme–Hme 125 |
| | | H6–Hme 1.3 |

resonances, with possible intermediate chemical shift labeling of one of the intervening carbon nuclei, using the coherence transfer pathway H6–C6–C5–Cme–Hme (Fig. 1B). The relatively large single bond $^1$H–$^{13}$C and $^{13}$C–$^{13}$C scalar interactions ensure fast coherence transfer across the pathway that comprises two H–C and two C–C bonds. The pulse scheme was designed to take into account the large dispersion of $^{13}$C chemical shifts in the pyrimidine base and the network of spin–spin scalar interactions among $^{13}$C, $^1$H, and $^{15}$N nuclei. The aromatic signals of pyrimidine C6 and C5 resonate around 137 and 110 ppm, respectively, while the thymine methyl carbons resonate upfield at around 12 ppm. Since the pyrimidine C4 resonances are located around 165–170 ppm, they must be manipulated in a way which prevents magnetization transfer to C4 via the large, single bond C5–C4 scalar coupling ($J_{C5,C4} \sim 55$ Hz). Due to the small chemical shift dispersion

(<1 ppm) of thymine C5 and thymine Cme resonances, the thymine C6 are used for the carbon chemical shift labeling. The chemical shifts and spin–spin coupling constants of proton and carbon nuclei in thymine are summarized in Table 1.

The pulse scheme of a three-dimensional **H6C6CCH(me)** experiment is shown in Fig. 2. The sequence starts with a refocused INEPT (*14*) transfer from H6 to C6 nuclei. The chemical shifts of the H6 resonances are encoded during the *t*1 evolution. A concatenated version (*15*) of an INEPT coherence transfer and a proton chemical shift evolution is used in order to minimize the number of 180° pulses. After the INEPT transfer, the carbon antiphase magnetization $2H6_zC6_x$ is allowed to refocus during the delay, 2δ, into in-phase $C6_y$ coherence which is subsequently labeled by its chemical shift during *t*2. In order to decouple the relatively large C6–C5 scalar interaction ($\sim$65 Hz), the $^{13}$C chemical shift labeling is accomplished using a constant time period matched to $1/J_{C6,C5}$. Simultaneous proton and carbon decoupling is achieved during the *t*2 evolution by shifting the proton and carbon 180° pulses separated by the delay $T$ in a synchronous manner and setting $T$ to $\frac{1}{2}J_{C6,C5} - \frac{1}{4}J_{H6,C6}$. The in-phase $C6_y$ magnetization is transferred to $C5_y$ in the next step by a carbon homonuclear TOCSY (*16, 17*). The full, in-phase coherence transfer is optimally attained by matching the TOCSY evolution to $\frac{1}{2}J_{C6,C5} \sim 7.7$ ms. During this step it is necessary to prevent magnetization transfer from C5 to C4. Since C4 resonances in pyrimidines are $\sim$50 ppm downfield from C5 resonances, this can be accomplished by application of a DIPSI-3 mixing sequence with an
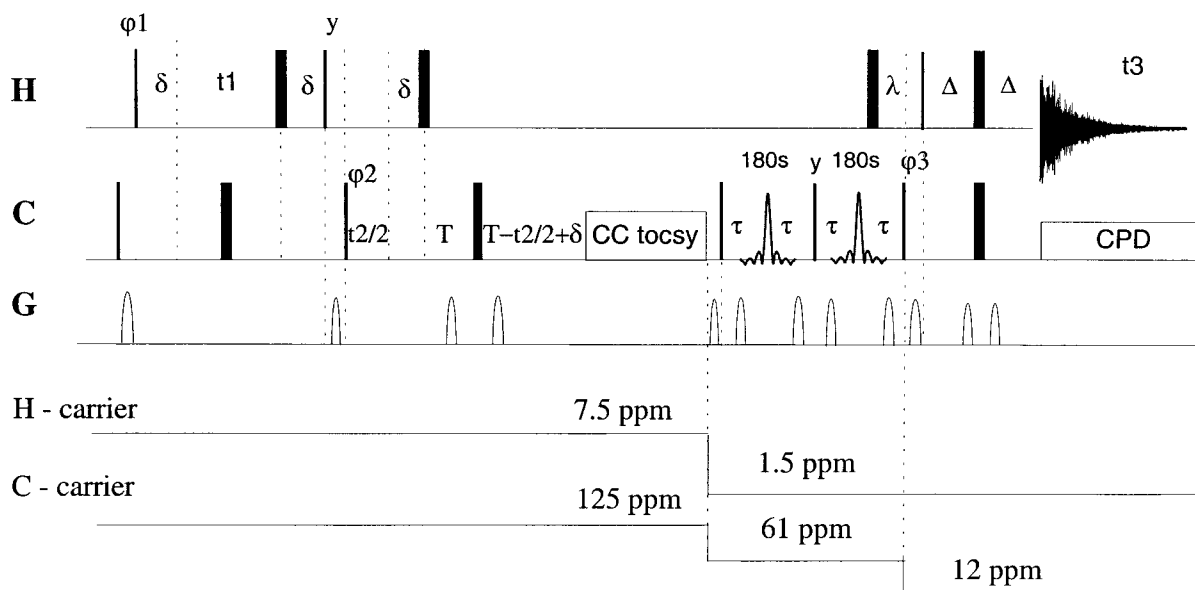


**FIG. 2.** Pulse scheme for the 3D HCCCH experiment . The thin and thick bars represent 90° and 180° pulses, respectively, applied along the *x*-axis unless specified otherwise. Delays are $T = 7$ ms, δ = 1.3 ms, τ = 5 ms, λ = 0.4 ms, and Δ = 2 ms. The phase cycling is φ1 = *x*, −*x*, φ2 = *x*, *x*, −*x*, −*x*, φ3 = 4*y*, 4(−*y*), and receiver = *x*, −*x*, −*x*, −*x*, *x*, *x*, −*x* combined with States–TPPI incrementation of φ1 and φ2 for quadrature detection in *t*1 and *t*2. Gradients of 800 µs followed by a 100 µs recovery delay are applied along the *z*-axis as spoiling and gradient echo pulses. Frequency switching of the proton and carbon carriers is as indicated, in order to optimize the sweep width in *f*1, *f*2, and *f*3 dimensions.
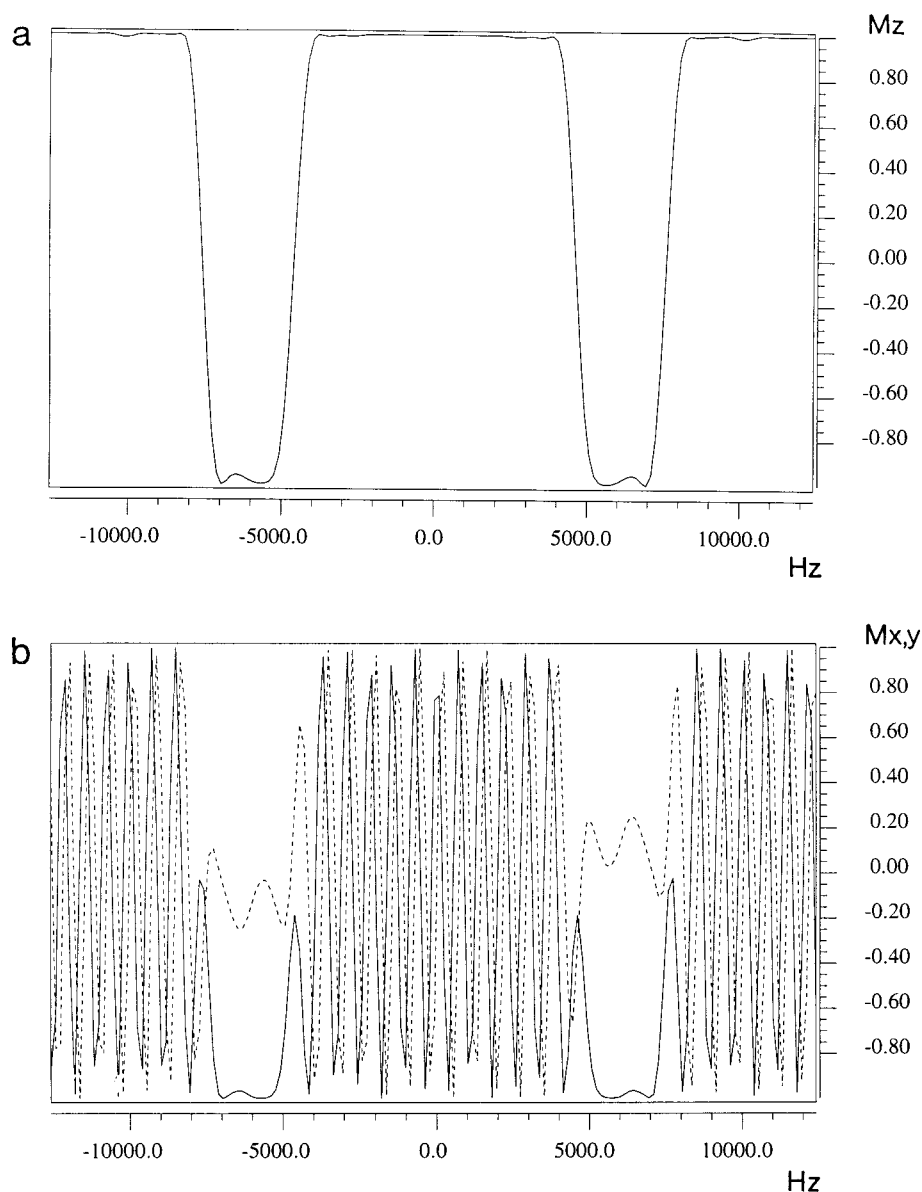
**FIG. 3.** Excitation profiles of the selective G3 180° pulse, where $t_{180} = 1.458$ ms and $\omega_m = 6173$ Hz: (a) $z$-profile and (b) $x$ (dashed lines) and $y$ (solid lines) profile.

RF field strength of 6.2 kHz and the carbon carrier set to the center of C5 resonances at 110 ppm. At the end of the single DIPSI-3 (*18*) supercycle an extra pulse is applied at the same power level. This pulse is used to compensate for the inhomogeneity of the RF field, and temporarily moves the C5$_y$ magnetization to the $z$-axis to allow for the carbon frequency switching in the subsequent step. The length of this pulse is easily optimized experimentally, and on our spectrometer (Bruker DRX500) it corresponds to a rotation of 65°.

The coherence transfer from C5 to Cme carbons is accomplished using a carbon–carbon refocused INEPT. In order to effectively suppress the C5–C4 scalar couplings while retaining the C5–Cme interactions, the INEPT is applied as a band

selective pulse sequence using shaped 180° pulses. Before the first 90$_x^\circ$ pulse, the carbon carrier is switched to $\omega_c = 61$ ppm to center the C5 and Cme regions at 110 and 12 ppm, respectively, and the carbon RF field is reset back to full power. During the first evolution period of $2\tau$, the C5$_y$ magnetization evolves into 2C5$_x$Cme$_z$ and is transferred by the subsequent 90$_y^\circ$ pulse into carbon methyl antiphase magnetization 2C5$_z$Cme$_x$. The 180° elements are applied during $2\tau$ as shaped pulses which simultaneously affect the C5 and Cme carbons, but in different ways. The 180° element in the middle of the first $2\tau$ evolution delay is used to refocus the C5 carbon chemical shifts at 110 ppm while simultaneously inverting the $z$-magnetization of Cme at 12 ppm. The corresponding shaped
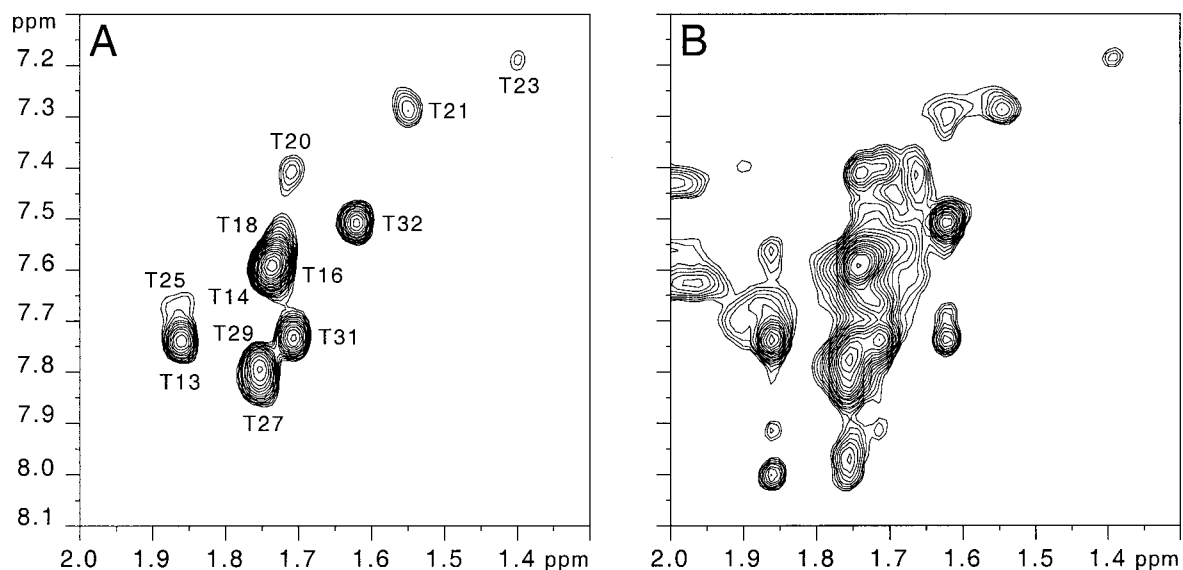
**FIG. 4.** Two-dimensional NMR spectra (500 MHz) of the H6–Hme correlations of the thymines in the 32 nucleotide uniformly $^{13}$C,$^{15}$N-labeled DNA intramolecular triplex d(AGAGAGAA<u>CCCC</u>TTCTCTCT<u>TATAT</u>CTCTCTT) (underlined bases are the loops) at 298 K obtained by HCCCH (A) and NOESY (B) experiments. The sample was 1.7 mM in 100 mM NaCl, 5 mM MgCl$_2$, pH 5.3 in 200 $\mu$l contained in a Shigemi NMR tube. The HCCCH spectrum was acquired with the following parameters: spectral width of 1.5 ppm in $f1$ and $f2$, using 64 and 256 complex points, respectively; 16 scans per $t1$ increment; and a total acquisition time of 30 min. The data were apodized with sine squared window functions shifted to 90° and 60° in $f1$ and $f2$, respectively. The final matrix size was 128 × 512. Parameters of the $^{13}$C-decoupled NOESY experiment: spectral width of 10 ppm in $f1$ and $f2$, using 635 and 1024 complex points, respectively; 64 scans per $t1$ increment; and a total acquisition time of 20 h. GARP $^{13}$C-decoupling was applied using an RF field strength of 3.85 kHz with the carrier positioned at 80 ppm. The data were apodized with sine squared window functions shifted to 75° and 65° in $f1$ and $f2$, respectively. The final matrix size was 1024 × 1024 points.

pulse must therefore perform satisfactorily both as a phase reversal and $z$-inversion pulse. This is achieved using a G3 Gaussian cascade waveform (*19*) for amplitude modulation of the 180° pulses with a cosinusoidal modulation (*20, 21*) $\omega_m$ = 49 ppm superimposed on the shaping envelope. The cosinusoidal modulation splits the excitation spectrum of the shaped pulse into two sidebands at $\omega_c \pm \omega_m$ with the excitation maxima at 110 and 12 ppm, respectively, in order to manipulate the C5 and Cme spins at their two distinct frequencies 98 ppm apart. The bandwidth of the G3 pulse was chosen to cover a range of 15–20 ppm, which is sufficiently narrow to avoid excitation at the frequency of C4 carbons.

The application of a cosine-modulated, phase reversal pulse in the center of the INEPT step requires some additional comment. In effect, the cosinusoidal modulation generates two "virtual" carriers at $\omega_c \pm \omega_m$. As a result, the transverse magnetizations of the C5 and Cme carbons are perfectly refocused in the corresponding rotating frames of reference at $\omega_c + \omega_m$ and $\omega_c - \omega_m$. However, during the application of the shaped pulse, the transverse components acquire an overall phase shift of $\Delta\phi = \pm\omega_m^* t_{180}^* 2\pi$ with respect to actual carrier $\omega_c$. In order to match the phase evolution of the 2C5$_x$Cme$_z$ magnetization to the phase of the 90$_y^\circ$ mixing pulse at $\omega_c$, the length $t_{180}$ of the 180° pulse has to be carefully adjusted to fulfill the condition $t_{180} = \mathbf{k}^*1/\omega_m$, where $\mathbf{k}$ is an integer. In this case, the overall phase shift $\Delta\phi$ becomes a multiple of $2\pi$ and can be safely neglected. To illustrate the

performance of a cosine modulated G3 Gaussian cascade, the results of computer simulations for $t_{180}$ = 1.458 ms and $\omega_m$ = 6173 Hz, corresponding to 49 ppm at 125.76 MHz, are shown in Fig. 3. As demonstrated, highly selective inversion and refocusing is obtained across the frequency bandwidths of $\omega_m \pm \frac{3}{2} t_{180}$, which corresponds to approximately $\omega_m \pm 8$ ppm from the carrier. A gradient echo is applied during the $2\tau$ evolution to discard the unwanted transverse components which are inevitably generated by non-selective 90° pulses. As a result, only the transverse magnetization refocused by the band selective G3 pulse forms an echo before the non-selective 90° mixing element. During the subsequent interval $2\tau$, the antiphase magnetization 2C5$_z$Cme$_x$ is allowed to refocus into the in-phase component Cme$_y$. The function of the cosine modulated G3 pulse is now reversed. The $z$-component of the C5 magnetization is inverted while the chemical shift evolution of Cme is refocused. At the same time, the antiphase magnetization with respect to the coupled protons of the methyl group 2Cme$_x$Hme$_z$ is generated by applying a 180° $^1$H pulse at the interval $\lambda$ before the CH INEPT transfer. This delay is matched to $2\lambda = 1/10\, J_{\text{Cme,Hme}}$ to maximize the transfer function 3 $\sin(2\pi J_{\text{Cme,Hme}}\lambda)\cos^2(2\pi J_{\text{Cme,Hme}}\lambda)$ of the reverse INEPT from carbon to the protons of the methyl group. After the antiphase magnetization refocusing, the methyl proton signal is detected with simultaneous $^{13}$C broadband decoupling. States–TPPI phase cycling (*22*) is applied both for $t1$ and $t2$ evolution, resulting in the final chemical shift modulation of Hme signals of the form

$\exp(-i\omega_{H6}t1)*\exp(-i\omega_{C6}t2)*\exp(-i\omega_{Hme}t3)$. In the two-dimensional version of the experiment the $^{13}$C chemical shift labeling is removed, resulting in H6–Hme correlations analogous to those in the homonuclear TOCSY.

The 2D and 3D versions of the experiment were applied to the 32 nucleotide intramolecular triplex. The DNA was enzymatically synthesized on a DNA template using Taq polymerase with uniformly $^{13}$C,$^{15}$N labeled dNTPs (*23*) as described elsewhere (*5*). The methyl-aromatic cross-peak regions of 2D HCCCH and $^{13}$C-decoupled NOESY spectra of the labeled triplex are shown in Fig. 4. The HCCCH spectrum was acquired in only 29 min while the NOESY spectrum required almost 20 h. Comparison of the two spectra allows the unambiguous distinction between intranucleotide and sequential NOE cross-peaks in the NOESY spectrum. The high sensitivity of the experiment should make it especially useful when applied to protein–DNA complexes, where it will make it possible to unambiguously identify the thymine methyl–H6 cross-peaks and distinguish them from other cross-peaks in the spectra.

## ACKNOWLEDGMENTS

## REFERENCES

*1.* T. Dieckmann and J. Feigon, Heteronuclear techniques in NMR studies of RNA and DNA, *Curr. Opin. Struct. Biol.* **4**, 745–749 (1994).

*2.* A. Pardi, "Multidimensional heteronuclear NMR experiments for structure determination of isotopically labeled RNA; (A. Pardi, Ed.), Vol. 261, pp. 350–380, Academic Press, San Diego (1995).

*3.* D. P. Zimmer and D. M. Crothers, NMR of enzymatically synthesized uniformly C13,N15-labeled DNA oligonucleotides, *Proc. Natl. Acad. Sci. U.S.A.* **92**, 3091–3095 (1995).

*4.* D. E. Smith, J. Y. Su, and F. M. Jucker, Efficient enzymatic synthesis of C-13,N-15-labeled DNA for NMR studies, *J. Biomol. NMR.* **10**, 245–253 (1997).

*5.* J. E. Masse, P. Bortmann, T. Dieckmann, and J. Feigon, Simple efficient protocol for enzymatic synthesis of uniformly 13C and 15N labeled DNA for heteronuclear NMR studies, *Nucleic Acids Res.* **26**, 2618–2624 (1998).

*6.* J. M. Louis, R. G. Martin, G. M. Clore, and A. M. Gronenborn, Preparation of uniformly isotope-labeled DNA oligonucleotides for NMR spectroscopy, *J. Biol. Chem.* **273**, 2374–2378 (1998).

*7.* G. Mer and W. J. Chazin, Enzymatic synthesis of region-specific isotope-labeled DNA oligomers for NMR analysis, *J. Am. Chem. Soc.* **120**, 607–608 (1998).

*8.* A. Ono, S. Tate, Y. Ishido, and M. Kainosho, Preparation and heteronuclear 2d NMR spectroscopy of a DNA dodecamer con-taining a thymidine residue with uniformly C-13-labeled deoxyribose ring, *J. Biomol. NMR.* **4**, 581–586 (1994).

*9.* M. Kainosho, Isotope labeling of macromolecules for structural determinations, *Nature Struct. Biol.* **4**, Supps., 858–871 (1997).

*10.* T. Szyperski, A. Ono, C. Fernandez, H. Iwai, S. Tate, K. Wuthrich, and M. Kainosho, Measurement of (*3*)J(C2′P) scalar couplings in a 17 kDa protein complex with C-13,N-15-Labeled DNA distinguishes the B-I and B-II phosphate conformations of the DNA, *J. Am. Chem. Soc.* **119**, 9901–9902 (1997).

*11.* A. Bax and D. G. Davis, MLEV-17-based two-dimensional homonuclear magnetization transfer spectroscopy, *J. Magn. Reson.* **65**, 355–360 (1985).

*12.* L. Braunschweiler and R. R. Ernst, Coherence transfer by isotropic mixing: Application to proton correlation spectroscopy, *J. Magn. Reson.* **53**, 521–528 (1983).

*13.* V. Sklenář and J. Feigon, Formation of a stable triplex from a single DNA strand, *Nature* **345**, 836–838 (1990).

*14.* G. A. Morris and R. Freeman, Enhancement of nuclear magnetic resonance signals by polarization transfer, *J. Am. Chem. Soc.* **101**, 760–762 (1979).

*15.* L. E. Kay, M. Ikura, and A. Bax, The design and optimization of complex NMR experiments. Application to a triple-resonance pulse scheme correlating H-alpha, NH, and N-15 chemical shifts in N-15-C-13-labeled proteins, *J. Magn. Reson.* **91**, 84–92 (1991).

*16.* G. M. Clore, A. Bax, P. C. Driscoll, P. T. Wingfield, and A. M. Gronenborn, Assignment of the side-chain $^1$H and $^{13}$C resonances of interleukin-1$\beta$ using double- and triple-resonance heteronuclear three-dimensional NMR spectroscopy, *Biochemistry* **29**, 8172–8184 (1990).

*17.* S. W. Fesik, H. L. Eaton, E. T. Olejniczak, and E. R. P. Zuiderweg, 2D and 3D NMR spectroscopy employing $^{13}$C–$^{13}$C magnetization transfer by isotropic mixing. Spin system identification in large proteins, *J. Am. Chem. Soc.* **112**, 886–888 (1990).

*18.* A. J. Shaka, C. J. Lee, and A. Pines, Iterative schemes for bilinear operators; application to spin decoupling, *J. Magn. Reson.* **77**, 274–293 (1988).

*19.* L. Emsley and G. Bodenhausen, Gaussian pulse cascades—New analytical functions for rectangular selective inversion and in-phase excitation in NMR, *Chem. Phys. Lett.* **165**, 469–476 (1990).

*20.* B. L. Tomlinson and H. D. W. Hill, Fourier synthesized excitation of nuclear magnetic resonance with application to homonuclear decoupling and solvent line suppression, *J. Chem. Phys.* **59**, 1775–1784 (1973).

*21.* R. Konrat, I. Burghardt, and G. Bodenhausen, Coherence transfer in nuclear magnetic resonance by selective homonuclear Hartmann–Hahn correlation spectroscopy, *J. Am. Chem. Soc.* **113**, 9135–9140 (1991).

*22.* D. Marion, M. Ikura, R. Tschudin, and A. Bax, Rapid recording of 2d NMR spectra without phase cycling—Application to the study of hydrogen exchange in proteins, *J. Magn. Reson.* **85**, 393–399 (1989).

*23.* R. T. Batey, M. Inada, E. Kujawinski, J. D. Puglisi, and J. R. Williamson, Preparation of isotopically labeled ribonucleotides for multidimensional NMR spectroscopy of RNA, *Nucleic Acids Res.* **20**, 4515–4523 (1992).